

LETTER TO THE EDITOR

Helical modulation of the electrostatic potential due to magnetic islands in toroidal plasma confinement devices

**G. Ciaccio¹, O. Schmitz², S. S. Abdullaev³, T. E. Evans⁴,
H. Frerichs², G. Spizzo¹, and R. B. White⁴**

¹ Consorzio RFX (CNR, ENEA, INFN, Università di Padova, Acciaierie Venete SpA), Corso Stati Uniti 4 - 35127 Padova (Italy)

² Department of Engineering Physics, University of Wisconsin - Madison, 1500 Engineering Drive, Madison, WI 53706

³ Institut für Energieforschung-Plasmaphysik, Association EURATOM-FZJ, Jülich, Germany

⁴ General Atomics, San Diego, California, USA

⁵ Plasma Physics Laboratory, Princeton University, P.O.Box 451, Princeton, New Jersey 08543

E-mail: giovanni.ciaccio@igi.cnr.it

Abstract.

The electrostatic response of a tokamak edge plasma to magnetic island with 4/1 poloidal/toroidal mode numbers is analyzed in direct comparison of measurements with the Hamiltonian guiding center code ORBIT. We find a strong correlation between the magnetic field topology in ion and electron velocity space and the poloidal modulation of the plasma potential measured. The ion and electron drifts yield a predominantly electron driven radial diffusion when approaching the island X-point while ion diffusivities are generally an order of magnitude smaller. This results in build up of a strong radial electric field structure pointing outward from the island O-point. An excellent agreement between measured and modeled plasma potential has been found. This shows that, in a tokamak edge plasma, a magnetic island can act as convective cell as pointed out by previous results. Here, we show for the first time that the particular drifts of electrons and ions in a 3D magnetic topology account for these effects. An analytical model for the radial particle diffusion is derived and it is shown that both, an ion and an electron diffusion dominated transport regime can exist which are known as ion and electron root solutions in stellarators. This finding and comparison to reversed field pinches shows that the role of magnetic islands as convective cells and hence as major radial particle transport drivers is generic to 3D plasma boundary layers of toroidal magnetic confinement devices.

PACS numbers: 52.20.Dq, 52.65.Cc

Plasma flows along magnetic field lines under conditions of spontaneous self-organization are a generic question in space and terrestrial plasma physics [1, 2]. In magnetically confined high temperature plasmas explored for future fusion energy production, such directed plasma flows are responsible for transport in the plasma edge. By this, the magnetic field topology in the plasma edge and the resulting transport characterizes the interface of the plasma to the surrounding neutral gas. One form of such self-organized 3D magnetic structures are magnetic islands. Field lines can be easily perturbed in a resonant way by magnetic field perturbations with the same mode structure as the rational surface of these field lines. In tokamaks, this form of resonant magnetic perturbation (RMP) is used to control plasma edge transport and stability [3, 4]. In the edge of all fusion devices, it has been observed that kinetic properties of the plasma, such as electron density and temperature [5, 6], electron pressure [7], connection length [8], in presence of 3D fields and magnetic chaos in the edge, show macroscopic modulations coherently with the symmetry of the dominant magnetic island. Moreover, it has been shown that magnetic islands influence the sign of the plasma flow, v , and the related radial electric field, E^r [7, 9, 10, 11].

The actual relation of these magnetic structures to plasma confinement and transport is an important question for fusion plasma research in particular as it has been demonstrated that magnetic islands in the plasma edge have a profound impact on plasma performance and plasma stability. At the RFP RFX-mod, for instance, a direct connection between a convective cell pattern and the empirical density limit (Greenwald limit) has been established [12, 13]. Island formation with impact on the particle confinement is also discussed as a key mechanism for stabilization of high confinement edge plasmas in tokamaks [14]. Finally, low-order rational surfaces in the periphery of stellarators make them prone to island formation which in some devices is used deliberately as exhaust layer between plasma core and the material wall elements around the plasma [15].

Since particle drift extent depends on Larmor radius, electrons stream along the field lines, while ions have larger mass and, hence, larger shift of the drift orbit from the flux surface. This results in an ambipolar field, with the same symmetry as the main magnetic island, to balance the drifts and ensure quasi-neutrality. On the basis of transport particle simulations performed through the guiding center (GC) Hamiltonian code ORBIT [16], a model of electrostatic potential was built up for the island resonating with poloidal/toroidal mode number $m/n = 0/1$ at the edge of RFX-mod [13], which reproduces the main features of E^r , such as amplitude and geometry along the toroidal angle φ .

In this Letter a comparative analysis is conducted for the first time for a tokamak with resonant magnetic perturbation fields applied. We study a circular shaped, high field side limited plasma at the TEXTOR tokamak [17], where a stochastic layer can be generated at the edge, by inducing RMPs through the Dynamic Ergodic Divertor (DED) [18]. The particle transport properties of the magnetic topology in the DED configuration $m/n = 12/4$ were analyzed using Poincaré plots and by calculating the parallel connection length, L_{\parallel} , for ions and electrons. The resulting L_{\parallel} map showed a radial and poloidal modulation, being footprints of the magnetic topology [19]. Results with ORBIT are consistent with maps of connection length made with GOURDON [20]. Previous results have pointed to the formation of island convective cells due to $E \times B$ flows around magnetic islands [21, 22, 23, 24]. Here, we show for the first time that ambipolar potentials, with the same symmetry as the magnetic island, due to differential drifts of ions and electrons in islands can account for the radial electric

fields responsible for these flows.

For this experiment, performed in the L-mode wall limited circular plasmas, the mode number resonant field $m/n = 3/1$ was used. The numerical interpretation was conducted using test particle transport simulations by means of the code ORBIT. We calculate the particle diffusion coefficients for electrons, D_e , and ions, D_i , and develop a model for the ambipolar potential, which describes the two-fluid, plasma response to the RMP. The modeled potential reproduces quite well measurements of plasma potential, performed with a Langmuir sweeping probe, inside of a $m/n = 4/1$ island which is formed close to the plasma edge. The results show that the development of an electrostatic potential is a general feature of magnetic islands resonating at the plasma edge: moreover, two possible ambipolar solutions are present, which resemble the “ion” and “electron-roots” typical of the E^r in stellarators [25]. A consequence is that modifying the T_e/T_i ratio can let the system flip from one solution to the other.

We consider a TEXTOR discharge with static RMP, in the $m/n = 3/1$ operational mode. In Fig. 1 we show the Poincaré plot of the vacuum magnetic field lines, superimposed to the helical 4/1 flux surfaces, $\psi_h^{(4,1)}$ [26], used for the computation domain and displayed as blue curves. We can recognize the characteristic magnetic topology of TEXTOR at the edge [20]: in the inner region the last main island chain composed by three conserved structures (green points), in the middle four *remnant islands* (purple points) and in the outermost region the *laminar flux tubes* embedded into the *stochastic fingers*. In Ref. [13] we presented the calculation of the

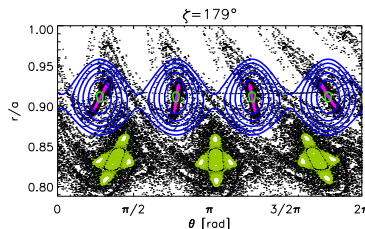


Figure 1: Poincaré plot of the vacuum magnetic field lines, superimposed to the helical 4/1 flux surfaces, $\psi_h^{(4,1)}$ (blue curves). The x-axis is the poloidal angle while the y-axis is the normalized radius.

particle diffusion coefficients, D , in between fixed points, O and X (OP and XP in the remainder of the Letter). Here, we propose again the result as it is complementary to the measurements of plasma potential and the modeled ambipolar potential, that we present below. D is calculated in an helical domain centered at the $q = 4$ resonance, ($r \approx 36$ cm), and bounded by $\psi_h^{(4,1)}$, highlighted in orange and light green in Fig. 1, respectively, which can be shifted from the OP towards the XP by varying the phase, ϕ , of $\psi_h^{(4,1)}$. We considered temperature $T_e = 90$ eV and $T_i = 100$ eV and thermal collisions with a background at density $n_e = 8.7 \times 10^{12}$ cm⁻³. These values are chosen to approximate the experiment conditions and calculated through the transport code EMC3-Eirene [28] in unperturbed conditions. The area of the domain is an *Archimedes' serpentine*, namely, a cyclic helical surface generated by the helical motion of a circle, whose area is $\mathcal{A} = 4\pi^2 b \sqrt{r_s^2 + R^2 q^2}$. In the formula, b is the radius of the circle normal to the helix, r_s is the resonance radius, and R the major radius.

D_e and D_i are shown in Fig. 2 as a function of the helical angle $u_{4,1} = 4\theta - \zeta + \phi$ [7].

Fig. 2 is adapted from Fig. 6 in Ref. [13]. Some D_e values have been corrected (D_e curve is smoother), but the overall result does not change. D_i is rather constant along the path ($\approx 0.1 \text{ m}^2/\text{s}$), while D_e is larger, with typical values in a stochastic field [27] ($0.6 \div 40 \text{ m}^2/\text{s}$). More important, D_e is strongly modulated along u (larger at the XP, lower at the OP), consistently with the L_{\parallel} simulations in Ref. [19], and the well-known experimental result that the laminar flux tubes (XP of the 4/1 island) are pathways of enhanced electron diffusion [20].

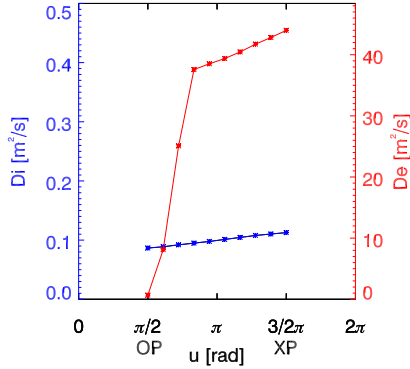


Figure 2: D_i and D_e values along the helical flux in between the OP and XP at $3\pi/2$. On the x-axis the helical angle $u = m\theta - n\zeta + \phi$.

Measurements of plasma potential have been done in the region of the 4/1 island by means of a fast insertable probe located at the low field side of the TEXTOR device [30]. The island is generated as a bifurcation with island opening at a given threshold DED current (1.8 kA for this configuration). Then the island, once generated, is moved poloidally by changing the phase of the DED current from shot to shot and in each shot one radial plunge of the fast reciprocating probe is taken. Fig. 3 shows a colored map of the measured plasma potential V_p in the (r, θ) plane, together with the helical flux surfaces $\psi_h^{(4,1)}$ and the magnetic field Poincaré map are overplotted to V_p . A very clear correlation of the V_p shape with the magnetic topology is found. In particular, the correlation is very strong in the region outside of the last closed flux surface (LCFS), while inside V_p does not follow exactly the flux surfaces. On the basis of the simulations of D and the measured V_p map, we find good reason to assume that the ambipolar potential Φ should possess the same geometry as the 4/1 island, similarly to the 0/1 and 1/7 island cases in RFX-mod [13, 7].

We now want to understand the link between the high electron diffusivity and the electric field structure. Therefore, we need to find a proper analytic form for Φ . To do that, we need to mix an experimental radial profile and simulation observations along θ , as previously done on RFX-mod [13]. In this way,

$$\Phi(\psi_p, \theta, \zeta) = \Phi_0 \left(f_1 + \frac{1}{2}(f_2 - f_1) \sin(-m\theta + n\zeta + \tilde{\phi}) \right), \quad (1)$$

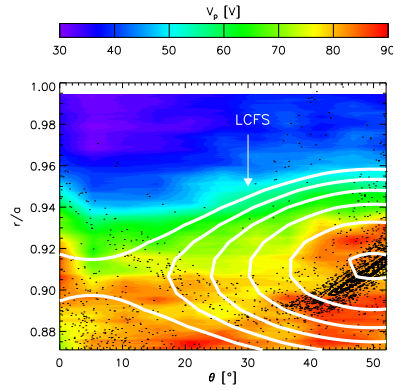


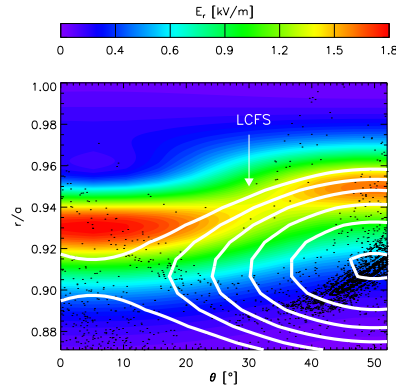
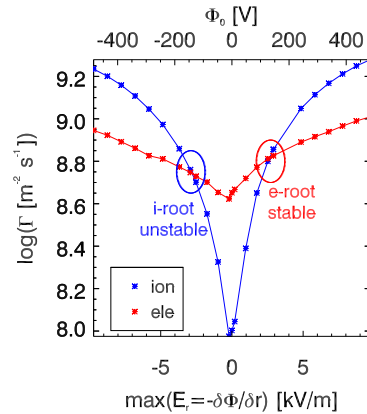
Figure 3: Map of the measured plasma potential V_p as a function of the poloidal angle θ and the normalized radius r . The helical flux surfaces $\psi_h^{(4,1)}$ (white contours) and the magnetic field Poincaré plot (points) are overlotted.

where

$$f_i(\psi_p) = V_{p,i}^{min} + \frac{1}{2}(V_{p,i}^{max} - V_{p,i}^{min}) \left(1 - \tanh\left(\frac{\psi_p - \psi_{p,i}}{\Delta\psi_{p,i}}\right) \right), \quad (2)$$

with $i = (1, 2)$. f_1 and f_2 are the curves fitting the radial profile of V_p (normalized to $\langle V_p \rangle \approx 85$ V in the OP) at the poloidal positions of the XP ($V_{p,1}^{min} = 0.35$, $V_{p,1}^{max} = 0.94$, $\psi_{p,1} = 0.0145$, $\Delta\psi_{p,1} = 0.0005$) and the OP ($V_{p,2}^{min} = 0.41$, $V_{p,2}^{max} = 1.00$, $\psi_{p,2} = 0.0148$, $\Delta\psi_{p,2} = 0.0003$), respectively. By setting $\Phi_0 = 90$ V (the maximum amplitude in the measurements) and $\tilde{\phi} = \phi$, i.e. the same phase of $\psi_h^{(4,1)}$, we obtain a model Φ , identical to the measured plasma potential. This is not surprising, considering the radial modulation of Φ which coincides by construction with measurements; but the fact that the poloidal dependence follows the geometry of the island is a striking new result in the tokamak. This behavior was already found instead in the reversed-field pinch RFX-mod [7], and in gyrokinetic simulations in Stellarators [31]. In Fig. 4, we map the $E^r = -\partial\Phi/\partial r$ amplitude together with the flux surfaces $\psi_h^{(4,1)}$ and magnetic field Poincaré plot, noting that E^r is modulated *both in the radial and in the poloidal directions*. In particular, a region of large positive E^r , along the LCFS, can be noticed. This is a confirmation of the well known presence of a positive E^r in the stochastic edge [32, 33, 34]. But, if we focus on this region, we can note also a modulation in the poloidal angle, strictly linked to the magnetic topology, too: E^r has a minimum in between the XP and the OP, and an absolute maximum in correspondence of the XP. On the contrary, right into the OP, E^r almost vanishes, which is consistent with LHD results [24, 29]. Therefore, the potential hill is located near the XP, where the electrons are preferably lost, as shown in Fig. 2 and in Ref. [19]. This rather complicated behavior of E^r should be accounted for when analyzing data in presence of RMPs [10, 35], since E^r varies both over r and θ .

As a final test, we check the ambipolarity of Φ by keeping $\tilde{\phi} = \phi$ (maximum

Figure 4: Map of the modeled E^r in the (θ, r) plane.Figure 5: Ion (blue) and electron (red) fluxes as a function of Φ_0 and the maximum E^r .

potential at the OP) and evaluating the electron and ion fluxes as a function of the maximum potential Φ_0 : this is the algebraic way of determining the ambipolar solution, used in the stellarator community [25]. To do this, we adapted ORBIT guiding center equations [16] to correctly express electron drifts. We evaluate fluxes at ψ_h , with source at $q = 4$. In Fig. 5 we plot the ion and electron fluxes as a function of Φ_0 and the maximum E^r . The two curves show two roots, similarly to stellarators [25]: an unstable ion-root at $E^r < 0$ (~ -150 V) and a stable electron-root at $E^r > 0$ (~ 120 V), where the latter is found for a positive potential consistently with the experimental findings (see Fig. 3). This shows that two solutions are possible: one with the potential hill (=maximum E^r) at the XP of the RMP (stable “electron root”, which is the solution found in experiment), and the other with the potential well at the OP (unstable, “ion root”). With the $T_e/T_i \sim 0.9$ ratio of TEXTOR, the electron root is favored, but in principle it is possible, by acting on the T_e/T_i ratio, to make the system flip to the ion root. This can be shown with ORBIT by varying T_e/T_i , increasing T_i , which in experiment condition would mean applying

ion cyclotron resonance heating (ICRH). We show the D_e/D_i ratio as a function of T_e/T_i in Fig. 6, with the diffusion coefficients calculated in the OP and XP. D_e/D_i decreases by increasing T_i similarly in the OP and XP, moving from the experiment condition pointed out by a vertical red line in the picture. In the OP the system flips to the ion root ($D_e/D_i < 0$) for $T_e/T_i \lesssim 0.5$. The opposite is seen experimentally

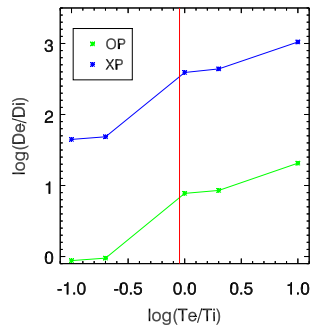


Figure 6: D_e/D_i as a function of T_e/T_i calculated in the OP and XP.

in stellarators, where the electron root can be induced actively by electron cyclotron resonance heating (ECRH) [25]. Indeed, experimental results in the ASDEX-U and FTU tokamaks show that disruptions can be mitigated by ECRH targeted on the 2/1 island [36]. We speculate that ECRH can modify the E^r distribution in the edge, and in this way the overall magnetohydrodynamics stability at the edge. In principle, this can be also a way of overcoming the density limit, which critically depends on the E^r pattern, at least in the RFP [12]. Finally, it should be worth doing experiments of ECRH in conjunction with RMP, to assess the role of E^r on plasma stability with respect to the so-called edge localized modes [14].

In summary, we analyzed the local radial particle transport along a helical path from the OP through the XP of an $m/n = 4/1$ remnant island, created near the edge of TEXTOR. Electron diffusion is strongly modulated (larger at the XP, lower at the OP), which requires a large electrostatic potential to ensure quasi-neutrality. We developed a 3D model for the ambipolar potential on the basis of the geometry of the remnant island: the resulting E^r shows a large positive value near the LCFS, confirming a well known result in the RMP tokamak community. The mechanism of ambipolarity shows two possible solutions ("roots"), which suggests a way of acting on the edge E^r through additional heating.

This project has received funding from the European Union Horizon 2020 research and innovation programme under grant agreement number 633053, and in part from the U.S. Department of Energy Grant DE-AC02-09CH11466.

References

- [1] V. P. Frolov, *Phys. Rev. D* **85**, 024020 (2012).
- [2] D. L. Meier, *New Astronomy Reviews* **47**, 667 (2003).
- [3] T. E. Evans, *et al.*, *Nature Phys.* **2**, 419 (2006).
- [4] O. Schmitz, *et al.*, *Phys. Rev. Lett.* **103**, 165005 (2009).
- [5] R. Moyer, *et al.*, *Nucl. Fusion* **52**, 123019 (2012).
- [6] H. Stoschus, O. Schmitz, *et al.*, *Nucl. Fusion* **52**, 083002 (2012).

- [7] N. Vianello, *et al.*, *Nucl. Fusion* **53**, 073025 (2013).
- [8] Y. Feng, *et al.*,
Plasma Phys. Control. Fusion **53**, 024009 (2011).
- [9] K. Kamiya, *et al.*, *Nucl. Fusion* **53**, 013003 (2013).
- [10] S. Mordijck, *et al.*, *Nucl. Fusion* **54**, 082003 (2014).
- [11] P. Scarin, *et al.*, *Nucl. Fusion* **51**, 073002 (2011).
- [12] M. Puiatti, *et al.*, *Nucl. Fusion* **51**, 073038 (2011).
- [13] G. Spizzo, *et al.*, *Phys. Plasmas* **21**, 056102 (2014).
- [14] P. Lang, *et al.*, *Nucl. Fusion* **53**, 043004 (2013).
- [15] H. Renner, *et al.*, *Nuclear Fusion* **40**, 1083 (2000).
- [16] R. B. White and M. S. Chance, *Physics of Fluids* **27**, 2455 (1984).
- [17] O. Neubauer, *et al.*, *Fus. Sci. Technol.* **47**, 76 (2005).
- [18] S. Abdullaev, “Magnetic stochasticity in magnetically confined fusion plasmas,” (Springer, Heidelberg, 2014).
- [19] G. Ciaccio, O. Schmitz, *et al.*, *Nucl. Fusion* **54**, 064008 (2014).
- [20] O. Schmitz, *et al.*, *Nucl. Fusion* **48**, 024009 (2008).
- [21] T.E. Evans, *et al.*, 14th EPS Madrid **11D**, 770 (1987).
- [22] S.C. McCool, *et al.*, *Nucl. Fusion* **30**, 167 (1990).
- [23] S. Takamura, *et al.*, *Phys. Fluids* **30**, 144 (1987).
- [24] K. Ida, *et al.*, *Nuclear Fusion* **44**, 290 (2004).
- [25] D. Hastings, *et al.*, *Nucl. Fusion* **25**, 445 (1985).
- [26] G. Ciaccio, M. Veranda, *et al.*, *Phys. Plasmas* **20**, 062505 (2013).
- [27] G. Spizzo, R. B. White, S. Cappello, and L. Marrelli,
Plasma Phys. Control. Fusion **51**, 124026 (2009).
- [28] M. Kobayashi, *Nucl. Fusion* **44**(6), S64 (2004).
- [29] K. Ida, *et al.*, *Phys. Rev. Lett.* **88**, 015002 (2001).
- [30] Y. Xu, *et al.*, *Nucl. Fusion* **47**, 1696 (2007).
- [31] J. M. García-Regaña, *et al.*, *Plasma Phys. Control. Fusion* **55**, 074008 (2013).
- [32] W. R. Hess, *et al.*,
Plasma Phys. Control. Fusion **37**, 951 (1995).
- [33] V. Rozhansky, *et al.*, *Nucl. Fusion* **50**, 034005 (2010).
- [34] Y. Xu, *et al.*, *Phys. Rev. Lett.* **97**, 165003 (2006).
- [35] J. Coenen, *et al.*, *Nucl. Fusion* **51**, 063030 (2011).
- [36] B. Esposito, G. Granucci, *et al.*, *Phys. Rev. Lett.* **100**, 045006 (2008).